

1. Semester project

Harmonic Oscillations in RLC-circuits and Torsion Pendulums

Written by

Nadine-Beatrice Cernat	-	nacer25@student.sdu.dk
Sofie Kiel Jørgensen	-	sojoe25@student.sdu.dk
Camilla Dybdal Carstensen	-	ccars25@student.sdu.dk
Marcus Grubbe Nesting	-	manes25@student.sdu.dk
Jakob Heilskov Dalgaard	-	jdalg25@student.sdu.dk

Supervisor

Torgom Yezekyan – ty@mci.sdu.dk

Physics & Technology
 University of Southern Denmark
 Odense, Denmark
 February 2026

1 Abstract

In this report, the different harmonic oscillations in a mechanical torsion pendulum and an electrical RLC-circuit were examined. The differential equations for the two systems were derived and solved both analytically and numerically using Euler's method, to display and examine the different damping types. To confirm these findings, experimental setups were used to perform oscillations.

Thereafter, the mechanical and electrical systems were compared, and it was found that the two differential equations describe the same motion for two different systems. This means that harmonic oscillations occur in both systems, although these systems are vastly different in setup.

It was found that the spring constant and the capacitor perform the same role of influence on the natural frequency of their corresponding systems.

Similarly the influence of the magnets on the damping of the mechanical oscillations corresponds to the role of resistor in the electrical system.

2 Use of generative artificial intelligence

Generative artificial intelligence has been used in this report to generate selected parts of MatLab code for data analysis and measurement processing. All AI generated outputs were critically evaluated to ensure a consistency with the established theory. In the case of inconsistencies between generated outputs and the theoretical expectations, further verification was achieved through guidance from supervisor and academic resources listed in references.

Contents

1 Abstract	1
2 Use of generative artificial intelligence	1
3 Introduction	3
3.1 Objective	3
3.2 Project boundaries	3
4 Theory	3
4.1 Mechanical differential equation	3
4.2 Electrical differential equation	8
5 Numerical approach	12
5.1 Euler's method	12
5.2 MATLAB code	13
6 Equipment	15
6.1 Mechanical	15
6.2 Electrical	16
7 Results	19
7.1 Mechanical results	19
7.2 Electronic results	24
7.3 Sources of error and measurement uncertainties	26
8 Analogy between the two systems	26
9 Conclusion	28
10 References	28

3 Introduction

This project focuses on harmonic oscillations in physical systems, specifically an electrical RLC system and a mechanical torsion pendulum. Harmonic oscillations occur commonly in nature and are essential to many technological devices. Understanding the principles of these oscillations and their mathematical fundamentals is essential for applications in both mathematics and physics.

Although physically different, both systems are described by the same linear second-order differential equation. The RLC circuit consists of a resistor (R), inductor (L), and capacitor (C) connected in series or parallel. When energy is supplied to the circuit, it oscillates between the capacitor's electric field and the magnetic field of the inductor, while the resistor damps the oscillation.

A torsional pendulum consists of a mounted disc attached to springs on either side, with one end fixed. When the disc is rotated from its equilibrium position, the springs produce a restoring torque proportional to the angular displacement, causing the system to undergo oscillatory rotational motion. In both cases, the systems exhibit oscillatory behavior around an equilibrium position.

3.1 Objective

The objective of this project is to model, measure experimentally, and compare driven and free oscillations in these two systems to illustrate the underlying theoretical and mathematical similarities. This is accomplished by:

- Deriving the mathematical equations describing the motion of the systems
- Conducting experiments based on these equations.
- Analyzing the experimental results and comparing measurements with the established theoretical model.
- Discussing the analogy and resemblance between the electrical and mechanical systems.

3.2 Project boundaries

This project focuses exclusively on free and driven oscillations, examining each type individually rather than as a combined solution. For the electrical system, only the RLC circuit in series is examined. The project has been developed collaboratively as a group effort, with the exception of the MATLAB programming, which was primarily handled by J. Dalgaard.

4 Theory

4.1 Mechanical differential equation

To establish the theoretical framework, the derivation begins with the second-order differential equation for the mechanical system. Initially the equation for a translational mechanical system is derived, after which it is translated into a rotational mechanical system, that is applicable to a torsion pendulum.

The forces acting on the mechanical system can be described with the following equation:

$$F_{res} = F_s + F_d + F_{ext} \quad (1)$$

Here, $F_s = F_{spring}$, $F_d = F_{damping}$, and $F_{ext} = F_{external}$. Each force can be looked at separately, starting with the spring force. The spring force is described using the following equation, where k is the spring constant:

$$F_s = -k \cdot x(t)$$

Next, the damping force is given by the following equation, where c is the damping constant:

$$F_d = -c \cdot v = -c \cdot \frac{dx(t)}{dt}$$

Lastly, the resultant force is given by Newton's 2. law as found in reference [1].

$$F_{res} = m \cdot a = m \cdot \frac{d^2x(t)}{dt^2}$$

If the system is let to oscillate on its own and the external forces acting on it are neglected, expression (1) can be written as follows:

$$0 = F_{res} - F_d - F_s \quad (2)$$

The definitions of each force can be substituted into equation (2), resulting in the following equation:

$$0 = m \cdot \frac{d^2x(t)}{dt^2} + c \cdot \frac{dx(t)}{dt} + k \cdot x(t) \quad (3)$$

Dividing by m on each term yields two constants, which can be used to describe the motion of the mechanical system.

$$0 = \frac{d^2x(t)}{dt^2} + \frac{c}{m} \cdot \frac{dx(t)}{dt} + \frac{k}{m} \cdot x(t)$$

The above expression holds true for the translational motion, but can be converted into rotational motion by substituting m with I (rotational inertia), $x(t)$ with $\theta(t)$ (angular displacement) as found in reference [1]. This gives us the following equation:

$$\frac{d^2\theta(t)}{dt^2} + \frac{c}{I} \cdot \frac{d\theta(t)}{dt} + \frac{k}{I} \cdot \theta(t) = 0 \quad (4)$$

Equation (4) shows that the system is described by two coefficients. The first one is the damping coefficient γ .

$$\gamma = \frac{c}{I} \quad (5)$$

The damping coefficient describes how the system responds to various damping effects, since it includes the impact of the damping force. The second constant is the square of the natural frequency ω_0 :

$$\omega_0^2 = \frac{k}{I}$$

This homogeneous differential equation is solved the same way as an ordinary quadratic polynomial with roots r .

$$ar^2 + br + c = 0$$

The coefficients are assigned $a = 1$, $b = \gamma$, and $c = \omega_0^2$. The quadratic formula is now used to solve for different cases of the discriminant d . The quadratic equation is as follows: $r = \frac{-b \pm \sqrt{D}}{2a}$ where $D = b^2 - 4ac$. For a case where $D > 0$, the roots become:

$$r_1 = \frac{-b + \sqrt{D}}{2a}, \quad r_2 = \frac{-b - \sqrt{D}}{2a}$$

Combining these roots gives the following general solution assuming that the answer is of the form e^{rt} , as found in reference [2]:

$$\theta(t) = Ae^{r_1 t} + Be^{r_2 t}$$

For case where $D = 0$, the answer has only one root:

$$r = \frac{-b}{2a}$$

With the general solution, found in reference [2]:

$$\theta(t) = Ae^{rt} + Bte^{rt}$$

Now, for the case where $D < 0$ the roots become a complex number and its conjugate:

$$\begin{aligned} r_1 &= \frac{-b + \sqrt{-1}\sqrt{-D}}{2a} = \frac{-b + i\sqrt{-D}}{2a} = \frac{-b}{2a} + i\frac{\sqrt{-D}}{2a} \\ r_2 &= \frac{-b - \sqrt{-1}\sqrt{-D}}{2a} = \frac{-b - i\sqrt{-D}}{2a} = \frac{-b}{2a} - i\frac{\sqrt{-D}}{2a} \end{aligned}$$

This gives the following general solution using Euler's formula to convert the imaginary exponential function into oscillating terms:

$$e^{iwt} = \cos(wt) + i \cdot \sin(wt)$$

We are only interested in the real part of the solution, so the following is done to remove the imaginary part:

$$\begin{aligned} &\frac{1}{2}\theta_1(t) + \frac{1}{2}\theta_2(t) \\ &= \frac{1}{2}e^{\frac{-b}{2a}t} \cdot \left(\cos\left(\frac{\sqrt{-D}}{2a}t\right) + i \cdot \sin\left(\frac{\sqrt{-D}}{2a}t\right) \right) + \frac{1}{2}e^{\frac{-b}{2a}t} \cdot \left(\cos\left(\frac{\sqrt{-D}}{2a}t\right) - i \cdot \sin\left(\frac{\sqrt{-D}}{2a}t\right) \right) \\ &= e^{\frac{-b}{2a}t} \cos\left(\frac{\sqrt{-D}}{2a}t\right) \end{aligned}$$

The general solution with arbitrary constants A and ϕ becomes:

$$\theta(t) = Ae^{\frac{-b}{2a}t} \cdot \cos\left(\frac{\sqrt{-D}}{2a}t + \phi\right)$$

Substituting the coefficients back in:

$$\theta(t) = Ae^{\frac{-\gamma}{2}t} \cdot \cos\left(\sqrt{\omega_0^2 - \frac{\gamma^2}{4}} \cdot t + \phi\right) \quad (6)$$

The angular frequency of this solution is now defined as:

$$\omega = \sqrt{\omega_0^2 - \frac{\gamma^2}{4}}$$

Since we are done understand the non-driven part of this oscillation, lets add an external force to our system in equation (4), it then becomes the following equation:

$$\tau_0 \cdot \cos(\omega t) = I \cdot \frac{d^2\theta(t)}{dt^2} + c \cdot \frac{d\theta(t)}{dt} + k \cdot \theta(t) \quad (7)$$

This equation can be solved by introducing a trial solution for the particular solution. Since the system is affected by the given force, a suitable trial solution is:

$$\theta_p(t) = A\cos(\omega t) + B\sin(\omega t) \quad (8)$$

Determining the constant A and B

Differentiating the trial solution gives:

$$\begin{aligned} \theta(t) &= A\cos(\omega t) + B\sin(\omega t) \\ \frac{d\theta(t)}{dt} &= -A\omega\sin(\omega t) + B\omega\cos(\omega t) \\ \frac{d^2\theta(t)}{dt^2} &= -A\omega^2\cos(\omega t) - B\omega^2\sin(\omega t) \end{aligned}$$

After differentiating, these expressions are substituted into equation (7), resulting in the following expression:

$$\begin{aligned} \tau_0\cos(\omega t) &= -IA\omega^2\cos(\omega t) - IB\omega^2\sin(\omega t) - cA\omega\sin(\omega t) + cB\omega\cos(\omega t) + kA\cos(\omega t) + kB\sin(\omega t) \\ &= (-IA\omega^2 + cB\omega + kA)\cos(\omega t) + (-IB\omega^2 - cA\omega + kB)\sin(\omega t) \end{aligned} \quad (9)$$

From equation (9), the following can be stated:

$$-IA\omega^2 + cB\omega + kA = \tau_0 \quad (10)$$

$$-IB\omega^2 - cA\omega + kB = 0 \quad (11)$$

These two statements must hold true in order for the system to be affected by the given force in equation (7). Now that the system has two equations with two unknowns, statements for the constants A and B can be determined. Starting with isolating the constant A in equation (11).

$$A = \frac{B(k - I\omega^2)}{c\omega} \quad (12)$$

Inserting expression (12) into equation (10) gives the following expression.

$$\tau_0 = \frac{B(k - I\omega^2)^2}{c\omega} + cB\omega$$

Solving for constant B gives the final expression for the constant:

$$B = \frac{\tau_0 c\omega}{(k - I\omega^2)^2 + (c\omega)^2} \quad (13)$$

The expression for B found in equation (13) is then used to simplify (12)

$$\begin{aligned} A &= \frac{\tau_0 \cdot c\omega}{(k - I\omega^2) + (c\omega)^2} \cdot \frac{k - I\omega^2}{c\omega} \\ &= \frac{\tau_0 \cdot c\omega \cdot (k - I\omega^2)}{(k - I\omega^2)^2 c\omega + (c\omega)^3} \\ &= \frac{\tau_0 \cdot (k - I\omega^2)}{(k - I\omega^2)^2 + (c\omega)^2} \end{aligned} \quad (14)$$

Using the expressions for A and B the particular solution can be written as follows:

$$\theta_p(t) = \left(\frac{\tau_0 \cdot (k - I\omega^2)}{(k - I\omega^2)^2 + (c\omega)^2} \right) \cdot \cos(\omega t) + \left(\frac{\tau_0 c\omega}{(k - I\omega^2)^2 + (c\omega)^2} \right) \cdot \sin(\omega t)$$

Determining Amplitude and Phase

The trial solution from equation (8) can be written differently to express the amplitude θ_0 and phaseshift ϕ

$$A\cos(\omega t) + B\sin(\omega t) = \theta_0\cos(\omega t - \phi) = \theta_0\cos(\omega t)\cos(\phi) + \theta_0\sin(\omega t)\sin(\phi)$$

From this expression, the constants B and A must be equal to:

$$A = \theta_0\cos(\phi), \quad B = \theta_0\sin(\phi)$$

To find an expression for the force τ_0 , it is beneficial to square all the terms, since it is expressed in both cosine and sine terms. This gives the following expressions:

$$A^2 = \theta_0^2\sin^2(\phi), \quad B^2 = \theta_0^2\cos^2(\phi)$$

By adding up these expressions for the constant A and B, we get the following:

$$\begin{aligned} A^2 + B^2 &= \theta_0^2(\sin^2(\phi) + \cos^2(\phi)) \\ A^2 + B^2 &= \theta_0^2(1) \\ \sqrt{A^2 + B^2} &= \theta_0 \end{aligned}$$

Using the expressions for A, equation (14), and B, equation (13), the amplitude, θ_0 , is given by:

$$\begin{aligned} \theta_0 &= \sqrt{\left(\frac{\tau_0 \cdot (k - I\omega^2)}{(k - I\omega^2)^2 + (c\omega)^2}\right)^2 + \left(\frac{\tau_0 \cdot c\omega}{(k - I\omega^2)^2 + (c\omega)^2}\right)^2} \\ &= \sqrt{\frac{\tau_0^2((k - I\omega^2)^2 + (c\omega)^2)}{((k - I\omega^2)^2 + (c\omega)^2)^2}} \\ &= \sqrt{\frac{\tau_0^2}{(k - I\omega^2)^2 + (c\omega)^2}} \\ \theta_0 &= \frac{\tau_0}{\sqrt{(k - I\omega^2)^2 + (c\omega)^2}} \end{aligned} \tag{15}$$

To find the angle ϕ between A and B , the tangent of the angle is taken:

$$\begin{aligned} \tan(\phi) &= \frac{B}{A} \\ \phi &= \arctan\left(\frac{B}{A}\right) = \arctan\left(\frac{\frac{\tau_0 \cdot c\omega}{(k - I\omega^2)^2 + (c\omega)^2}}{\frac{\tau_0 \cdot (k - I\omega^2)}{(k - I\omega^2)^2 + (c\omega)^2}}\right) \\ \phi &= \arctan\left(\frac{c\omega}{k - I\omega^2}\right) \end{aligned}$$

When considering the phase difference between the system and the applied force, there are 3 points of interest: When the angle between the system and the applied force is 0° , when there is a 90° difference, and the last one is when there is a 180° difference.

This means that when there is a 0° difference, the system and the applied force are parallel to each other, whilst a 180° phase difference means they are directly opposite to each other.

When there is a 90° difference is where the resonance occurs. If the system oscillates with a cosine function, and the velocity is described by differentiating this function, this leads to a $-\sin$ function. The phase difference between these two functions is $\frac{\pi}{2}$ or 90° . This means that when there is a phase difference of $\frac{\pi}{2}$ between the applied force and the oscillations of the system, the applied force creates constructive interference with the velocity of the system. This leads to resonance.

4.2 Electrical differential equation

In order to derive the differential equation for the electrical circuit, we start by describing the voltage across each component. This total voltage across the circuit, when the components are connected in series, is the sum of the voltages across the resistor, inductor, and capacitor:

$$v_s = v_R + v_L + v_C \quad (16)$$

We can analyze each component separately. The voltage through the resistor is given by Ohm's law:

$$v_R = R \cdot i$$

Therefore, the voltage through the resistor over time is given by the following.

$$v_R(t) = R \cdot i(t) \quad (17)$$

The voltage over the inductor as a function of time as found in reference [3] is given by:

$$\begin{aligned} \int_{t_0}^t v_L(t) dt &= i(t) \cdot L - i(t_0) \\ v_L(t) &= L \cdot \frac{di(t)}{dt} - \frac{di(t_0)}{dt} = L \cdot \frac{di(t)}{dt} \end{aligned} \quad (18)$$

The voltage over the capacitor as found in reference [3] is given by:

$$v_C(t) = \frac{1}{C} \cdot \int_{t_0}^t i(t) dt + v(t_0) \quad (19)$$

Combining these expressions ((17),(18),(19)) in (16) we obtain the following equation for the total voltage:

$$v(t) = R \cdot i(t) + L \cdot \frac{di(t)}{dt} + \frac{1}{C} \int_{t_0}^t i(t) dt + v(t_0)$$

Differentiating the entire equation with respect to time t, we obtain:

$$\frac{dv(t)}{dt} = R \cdot \frac{di(t)}{dt} + L \cdot \frac{d^2i(t)}{dt^2} + \frac{1}{C} \cdot i(t) \quad (20)$$

To isolate the second-order derivative term, we divide the entire equation by the inductance L:

$$\frac{1}{L} \frac{dv(t)}{dt} = \frac{d^2i(t)}{dt^2} + \frac{R}{L} \cdot \frac{di(t)}{dt} + \frac{1}{LC} \cdot i(t)$$

If we disconnect the outer source and allow the components to oscillate without external influence, the differential equation would be of the second-order and linear homogeneous:

$$\frac{d^2i(t)}{dt^2} + \frac{R}{L} \frac{di(t)}{dt} + \frac{1}{LC} i(t) = 0$$

This equation describes the natural response of the RLC circuit, where the behavior of the current, $i(t)$ is determined only by the internal dynamics of the components.

However, if we were to introduce an external AC voltage source, $v_s = V_0 \cos(\omega t)$, the behavior of the circuit changes significantly. This external forcing term causes the circuit to respond at the frequency of the driving force, ω , rather than its natural frequency.

For a sinusoidal driving voltage $v_s(t) = V_0 \cos(\omega t)$, the derivative of the source voltage is:

$$\frac{dv_s(t)}{dt} = -\omega V_0 \sin(\omega t).$$

By substituting this into equation (20), the differential equation for the driven RLC circuit becomes:

$$L \cdot \frac{d^2 i(t)}{dt^2} + R \cdot \frac{di(t)}{dt} + \frac{1}{C} \cdot i(t) = -\omega V_0 \sin(\omega t). \quad (21)$$

To find the particular solution of the differential equation for the driven RLC circuit we use the method of undetermined coefficients. Since the right side of the equation is a sinusoidal voltage function, we assume a particular solution of the form:

$$i_p(t) = A \cos(\omega t) + B \sin(\omega t). \quad (22)$$

Calculating the first and second derivatives of the particular solution $i_p(t)$, we get:

$$\frac{di_p(t)}{dt} = -A\omega \sin(\omega t) + B\omega \cos(\omega t)$$

And:

$$\frac{d^2 i_p(t)}{dt^2} = -A\omega^2 \cos(\omega t) - B\omega^2 \sin(\omega t)$$

Substituting these derivatives and the particular solution $i_p(t)$ into the differential equation for the driven RLC circuit (21):

$$\begin{aligned} L(-A\omega^2 \cos(\omega t) - B\omega^2 \sin(\omega t)) + R(-A\omega \sin(\omega t) + B\omega \cos(\omega t)) \\ + \frac{1}{C}(A \cos(\omega t) + B \sin(\omega t)) = -\omega V_0 \sin(\omega t). \end{aligned}$$

By combining the terms involving $\cos(\omega t)$ and $\sin(\omega t)$, we get:

$$\left(-LA\omega^2 + RB\omega + \frac{A}{C} \right) \cos(\omega t) + \left(-LB\omega^2 - RA\omega + \frac{B}{C} \right) \sin(\omega t) = -\omega V_0 \sin(\omega t).$$

Determining the Constants A and B

To determine the constants A and B , we equate the coefficients of $\cos(\omega t)$ and $\sin(\omega t)$ on both sides of the differential equation, which gives us the following two equations:

$$\begin{aligned} -LA\omega^2 + RB\omega + \frac{A}{C} &= 0 \\ -LB\omega^2 - RA\omega + \frac{B}{C} &= -\omega V_0 \end{aligned}$$

Which can be rewritten as:

$$A \left(\frac{1}{C} - L\omega^2 \right) + B(R\omega) = 0 \quad (23)$$

$$-A(R\omega) + B \left(\frac{1}{C} - L\omega^2 \right) = -\omega V_0 \quad (24)$$

From equation (23), we can isolate A :

$$\begin{aligned} A \left(\frac{1}{C} - L\omega^2 \right) &= -B(R\omega) \\ A &= -B \frac{R\omega}{\left(\frac{1}{C} - L\omega^2 \right)} \end{aligned} \quad (25)$$

Thus, A from (25) can be substituted into equation (24) to isolate B :

$$\begin{aligned} -\left(-B \frac{R\omega}{\left(\frac{1}{C}-L\omega^2\right)}\right)(R\omega) + B \left(\frac{1}{C}-L\omega^2\right) &= -\omega V_0 \\ B \frac{(R\omega)^2}{\left(\frac{1}{C}-L\omega^2\right)} + B \left(\frac{1}{C}-L\omega^2\right) &= -\omega V_0 \end{aligned}$$

Factoring out B :

$$B \left(\frac{(R\omega)^2}{\left(\frac{1}{C}-L\omega^2\right)} + \left(\frac{1}{C}-L\omega^2\right) \right) = -\omega V_0$$

Combining the terms inside the parentheses:

$$B \left(\frac{(R\omega)^2 + \left(\frac{1}{C}-L\omega^2\right)^2}{\left(\frac{1}{C}-L\omega^2\right)} \right) = -\omega V_0$$

Isolating B :

$$B = \frac{-\omega V_0}{\left(\frac{(R\omega)^2 + \left(\frac{1}{C}-L\omega^2\right)^2}{\left(\frac{1}{C}-L\omega^2\right)}\right)} = \frac{-\omega V_0 \left(\frac{1}{C}-L\omega^2\right)}{(R\omega)^2 + \left(\frac{1}{C}-L\omega^2\right)^2}$$

Substituting this expression for B into the equation for A :

$$A = -\left(\frac{-\omega V_0 \left(\frac{1}{C}-L\omega^2\right)}{(R\omega)^2 + \left(\frac{1}{C}-L\omega^2\right)^2}\right) \frac{R\omega}{\left(\frac{1}{C}-L\omega^2\right)}$$

Simplifying the expression:

$$A = \left(\frac{\omega V_0}{(R\omega)^2 + \left(\frac{1}{C}-L\omega^2\right)^2}\right) R\omega$$

Thus, the final expression for A is:

$$A = \frac{V_0 R \omega^2}{(R\omega)^2 + \left(\frac{1}{C}-L\omega^2\right)^2}.$$

The particular solution is then given by substituting A and B into equation (22):

$$i_p(t) = \left(\frac{V_0 R \omega^2}{(R\omega)^2 + \left(\frac{1}{C}-L\omega^2\right)^2}\right) \cos(\omega t) + \left(\frac{-\omega V_0 \left(\frac{1}{C}-L\omega^2\right)}{(R\omega)^2 + \left(\frac{1}{C}-L\omega^2\right)^2}\right) \sin(\omega t)$$

Determining Amplitude and Phase

To derive the amplitude, I_0 , the trigonometric identity for a linear combination of sine and cosine functions for equation (22) can be used. This allows us to simplify the equation into a single sinusoidal function:

$$A \cos(\omega t) + B \sin(\omega t) = I_0 \cos(\omega t - \phi)$$

The right-hand side of the equation can then be expanded using the difference identity of cosine:

$$I_0 \cos(\omega t - \phi) = I_0 \cos(\phi) \cos(\omega t) + I_0 \sin(\phi) \sin(\omega t)$$

By comparing coefficients of $\cos(\omega t)$ and $\sin(\omega t)$ on both sides, we get:

$$A = I_0 \cos(\phi)$$

$$B = I_0 \sin(\phi)$$

Squaring both equations and adding them together:

$$A^2 + B^2 = I_0^2 (\cos^2(\phi) + \sin^2(\phi))$$

Since $\cos^2(\phi) + \sin^2(\phi) = 1$:

$$A^2 + B^2 = I_0^2$$

Taking the square root of both sides, we get the amplitude:

$$I_0 = \sqrt{A^2 + B^2} \quad (26)$$

Substituting the expressions for A and B , the amplitude I_0 becomes:

$$I_0 = \sqrt{\left(\frac{V_0 R \omega^2}{(R\omega)^2 + (\frac{1}{C} - L\omega^2)^2} \right)^2 + \left(\frac{-\omega V_0 (\frac{1}{C} - L\omega^2)}{(R\omega)^2 + (\frac{1}{C} - L\omega^2)^2} \right)^2}$$

Since both terms inside the square root have the same denominator, the amplitude I_0 can be rewritten as:

$$I_0 = \sqrt{\frac{(V_0 R \omega^2)^2 + (-\omega V_0 (\frac{1}{C} - L\omega^2))^2}{((R\omega)^2 + (\frac{1}{C} - L\omega^2)^2)^2}}$$

Factor out $V_0^2 \omega^2$ from the numerator:

$$I_0 = \sqrt{\frac{V_0^2 \omega^2 (R^2 \omega^2 + (\frac{1}{C} - L\omega^2)^2)}{((R\omega)^2 + (\frac{1}{C} - L\omega^2)^2)^2}}$$

Since the term inside the brackets of the numerator is the same as the denominator without the square, we can simplify it as:

$$I_0 = \sqrt{\frac{V_0^2 \omega^2}{((R\omega)^2 + (\frac{1}{C} - L\omega^2)^2)}}$$

Taking the square root of the numerator and the denominator:

$$I_0 = \frac{V_0 \omega}{\sqrt{(R\omega)^2 + (\frac{1}{C} - L\omega^2)^2}}$$

Factoring out ω in the numerator, the final expression for the amplitude becomes:

$$I_0 = \frac{V_0}{\sqrt{R^2 + (\omega L - \frac{1}{\omega C})^2}}$$

The phase shift ϕ of a sinusoidal function can be determined using the arctangent of the ratio of B to A . The phase shift ϕ is given by:

$$\phi = \arctan \left(\frac{B}{A} \right) \quad (27)$$

Substituting the expressions for A and B into the formula:

$$\phi = \arctan \left(\frac{\frac{-\omega V_0 (\frac{1}{C} - L\omega^2)}{(R\omega)^2 + (\frac{1}{C} - L\omega^2)^2}}{\frac{V_0 R \omega^2}{(R\omega)^2 + (\frac{1}{C} - L\omega^2)^2}} \right)$$

Since the denominators of A and B are the same, they cancel out:

$$\phi = \arctan \left(\frac{-\omega V_0 \left(\frac{1}{C} - L\omega^2 \right)}{V_0 R \omega^2} \right)$$

The expression can then be simplified by canceling out common terms in the numerator and the denominator:

$$\phi = \arctan \left(\frac{-\left(\frac{1}{C} - L\omega^2 \right)}{R\omega} \right)$$

This expression provides the phase shift of the current relative to the source voltage in the RLC circuit.

After identifying methods for finding the angle and amplitude, the chosen components for the electrical circuit accounted for in section 6.2 were then analyzed. This is accomplished by examining equation (6), where the known parameters from the electrical circuit are substituted into the complex part of the expression. Thereby getting the following equations:

$$\begin{aligned} \frac{\sqrt{\frac{4}{LC} - (\frac{R}{L})^2}}{\sqrt{4}} &\Leftrightarrow \sqrt{\frac{\frac{4}{LC} - (\frac{R}{L})^2}{4}} \\ \sqrt{\frac{1}{LC} - \frac{R^2}{4L^2}} &\Leftrightarrow \sqrt{\frac{1}{LC} - (\frac{R}{2L})^2} \end{aligned} \quad (28)$$

Equation (28) has the units [$\frac{\text{rad}}{\text{s}}$]. This can be converted into frequency with units [Hz] by dividing with 2π , resulting in the following equation:

$$\frac{\sqrt{\frac{1}{LC} - (\frac{R}{2L})^2}}{2\pi}$$

By substituting the component values, two numerical results are obtained. If these values are comparable, damping has a significant effect on the system. If the values are not comparable, larger damping would be required to noticeably affect the system.

$$\frac{\sqrt{2.12 \cdot 10^7 - 3.36 \cdot 10^6}}{2\pi}$$

Where $\frac{1}{LC} = 2.12 \cdot 10^7$ and $(\frac{R}{2L})^2 = 3.36 \cdot 10^6$. Since these values are comparable by a factor of 10, damping has a large effect on the system. Based on this result, only small changes in damping should be applied to the electrical circuit to avoid noticeable differences in the circuit's behavior.

5 Numerical approach

Another way to solve these ordinary differential equations is by using a numerical method to approximate the solutions by iteration. In this project, Euler's method is utilized to quickly and conveniently plot and analyze these oscillations in MATLAB.

5.1 Euler's method

Euler's method uses linear approximation to estimate the solution of first order differential equations. The method starts with having a known starting point $y(x_0) = y_0$ and a given equation $f(x, y(x))$

that satisfies the relationship: $y'(x) = \frac{dy}{dx} = f(x, y(x))$. Now, if y is differentiable, we use linear approximation to estimate the value of y , when x is increased by a tiny amount h :

$$y(x_0 + h) \approx y(x_0) + h \cdot f(x_0, y_0)$$

As is evident, the error of this approximation is directly proportional to h . When we let $h \rightarrow 0$, then:

$$y(x_0 + h) = y(x_0) + h \cdot f(x_0, y_0), h \rightarrow 0$$

When this process is repeated many times with each new iteration using the previous estimate $y(x_0 + h)$ as $y(x_0)$, the following recursive formulas describe the process:

$$x_{n+1} = x_n + h$$

$$y_{n+1} = y_n + h \cdot f(x_n, y_n)$$

When dealing with second order ODE's, you can convert them into a system of two first order ODE's. Suppose that now you have an equation of the form $f(x, y(x), y'(x))$ that satisfies $y''(x) = f(x, y(x), y'(x))$. Notice that the process now requires two known starting points $y(x_0) = y_0$ and $y'(x_0) = y'_0$

$$y'_{n+1} = y'_n + h \cdot f(x_n, y_n, y'_n)$$

$$y_{n+1} = y_n + h \cdot y'_n$$

5.2 MATLAB code

To solve our differential equations in MatLab, we arrange them in the form of Euler's recursive formulas and find new estimated solution points by iteration in a for-loop. The for-loops with the homogeneous and particular equation are seen in figures in 1a and 1b. The code is based on the translative differential equation (3).

```
for i = 1:length(t)-1
    ddxdt = -(d/m)*dxdt(i) - (k/m)*x(i);
    x(i+1) = x(i) + dxdt(i) * dt;
    dxdt(i+1) = dxdt(i) + ddxdt * dt;
end
```

(a) For-loop: Homogeneous solution

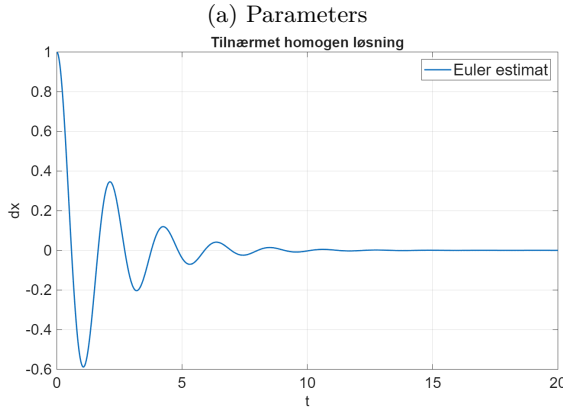
```
for i = 1:length(t)-1
    F = A * cos(w * t(i)); %ydre kraft
    %eulermetode som før
    ddxdt_p = (F/m) - (d/m)*dxdt_p(i) - (k/m)*x_p(i);
    x_p(i+1) = x_p(i) + dxdt_p(i)*dt;
    dxdt_p(i+1) = dxdt_p(i) + ddxdt_p*dt;
end
```

(b) For-loop: Particular solution

Figure 1: Screenshots of the MATLAB code for (a) the homogeneous solution and (b) the particular.

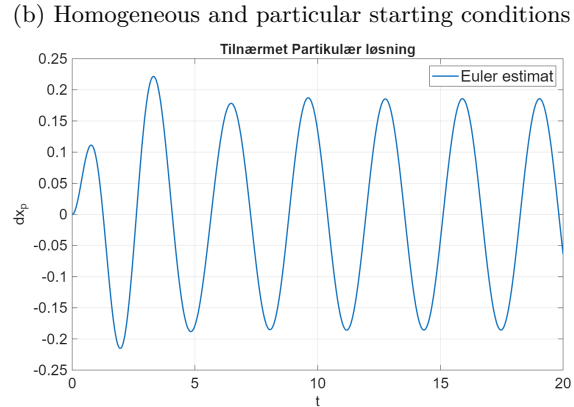
The homogeneous starting conditions are chosen as to release the system motion from a given displacement from the equilibrium. The starting velocity condition is therefore set to zero and the starting position condition depends on where the system is released from. The particular starting conditions are chosen so that all motion caused by the outer force is isolated. Choosing both to be zero causes initially $a = \frac{F}{m}$, which is the desired particular motion. The parameters are chosen arbitrarily for now and the time step small enough compared to the frequency of the oscillations and desired accuracy. This is seen in figure 2.

```
m = 1; % I or L(inductans)
d = 1; % Damping
k = 9; % or 1/C
dt = 0.00001; %time step
t = 0:dt:20; %time span
A = 1; % Force Amplitude
w = 2; % Force frequency
```



(c) Estimated homogeneous solution

```
% Startbetingelser
x = zeros(size(t)); x(1) = 1;
dxdt = zeros(size(t)); dxdt(1) = 0;
% Partikulære Startbetingelser
x_p = zeros(size(t)); x_p(1) = 0;
dxdt_p = zeros(size(t)); dxdt_p(1) = 0;
```



(d) Estimated particular solution

Figure 2: Screenshots of the MATLAB code (a) the parameters used in the numerical approach, (b) the starting points for Eulers method, (c) an estimation of a homogeneous solution and (d) an estimation of a particular solution.

A resonance plot can also be made by calculating particular solutions for a range of different driving frequencies and plotting the resulting amplitudes after motion has become regular. This is because the particular solution becomes the full solution after the homogeneous part has died out. A phase response curve can also be made by fitting the regular motion to a cosine model with a phase shift with respect to zero (driving phase shift) for each iteration. This is seen in figure 3.

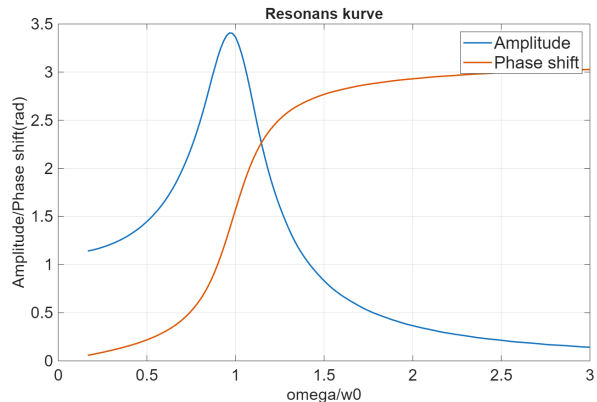
```
for h = 1:length(omega)
  faseforhold(h) = omega(h)/w0; % Frekvensratio

  % Partikulær løsning igen(samme som steady state efter et stykke tid)
  for i = 1:length(t)-1
    F = A * cos(omega(h) * t(i));
    ddxdt = (F/m) - (d/m)*dxdt(i) - (k/m)*x(i);

    x(i+1) = x(i) + dxdt(i)*dt;
    dxdt(i+1) = dxdt(i) + ddxdt*dt;
  end
  %vi skal have x-værdier efter x_p er blevet regelmæssig
  x_steady = x(round(length(x)/2):end);
  t_steady = t(round(length(t)/2):end);
  amplitude(h) = (max(x_steady) - min(x_steady))/2;

  %cos fit
  fit = lsqcurvefit(@(p, t) p(1) * cos(omega(h)*t - p(2)), ...
    [(max(x_steady)-min(x_steady))/2, 0], t_steady, x_steady);
  if fit(1) < 0
    fit(2) = fit(2) + pi;
  end
  fasevinkel(h) = fit(2);
end
fasevinkel = unwrap(fasevinkel);
```

(a) For loop: Frequency sweep



(b) Resonance and phase response curve

Figure 3: Resonant frequency curve for numerical approach. (a) The code used to generate the frequency sweep and (b) the graph of the resonance and phase response.

It is apparent here that the phase shift between the driving and particular frequency approaches zero below the natural frequency, meaning that they are roughly in phase. It is $\frac{\pi}{2}$ at the natural frequency

and π out of phase for driving frequencies above the natural frequency. The width of the phase shift transition broadens as damping increases. The resonance peak happens when the driving frequency is in phase with the particular frequency, which is affected by damping. Damping makes the system respond to a wider range of frequencies, but in lower magnitude. In other words, the resonance peak moves to the left, and broadens and flattens for higher damping values and can only ever be as high as the natural frequency of the system.

6 Equipment

6.1 Mechanical

The experiments for the mechanical system were performed using the setup shown in figure 4.

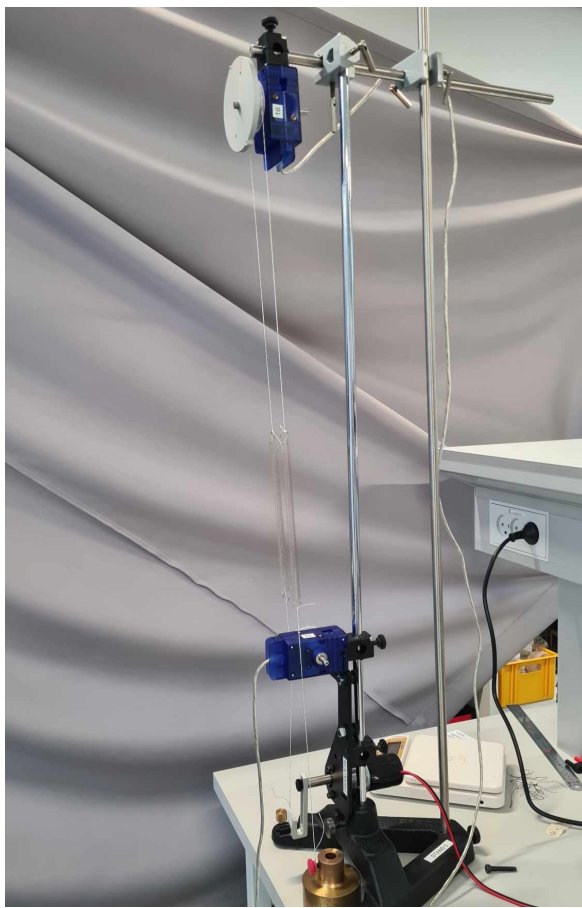


Figure 4: The torsion pendulum setup, with the two motors, two springs and the disc, without any added weight. The magnet, used for damping the disc, is fixed on the upper motor, behind the disc.

To obtain the measurements for the mechanical torsion pendulum, the software Pasco Capstone was used as a data acquisition tool. Capstone also made it possible to record data for the driven oscillations.

For the mechanical system, the following parameters were changed:

- Damping, by using different magnets and changing their distance from the disc.
- Inertia of the disc by adding weight.

Three magnets of different magnitudes were used to change the damping. Furthermore, the distance between the disc and magnet could be changed, providing a wider range of damping conditions. To adjust the inertia of the disc, a weight of 20 *gram* and a weight of 50 *gram* were added. The resulting inertia values are shown in table 1.

Table 1: Inertia calculated for the disc with no added weight, with approximately 20 gram added, and 50 gram added.

Total weight [kg]	Inertia [$kg \cdot m^2$]
0,1223	$I = \frac{1}{2} \cdot 0,1223 kg \cdot (0,0475m)^2 = 0,000014 kg \cdot m^2$
0,1423	$I = \frac{1}{2} \cdot 0,1423 kg \cdot (0,0475m)^2 = 0,00016 kg \cdot m^2$
0,1723	$I = \frac{1}{2} \cdot 0,1723 kg \cdot (0,0475m)^2 = 0,000194 kg \cdot m^2$

To determine the spring constant, the length of the spring was first measured without any attached mass. Afterwards, the following masses were added: 19.8*g*, 39.9*g* and 49.9*g*. For each mass, the change in spring extension was measured, resulting in three data points. A regression analysis was then executed, with the slope of the resulting line representing the spring constant of the spring.

This procedure was carried out for both springs, and got the same value.

$$\text{Spring constant} = 0,0208 \frac{N}{m}$$

6.2 Electrical

The experiments for the electrical circuit were performed using the setup shown in figure 5.

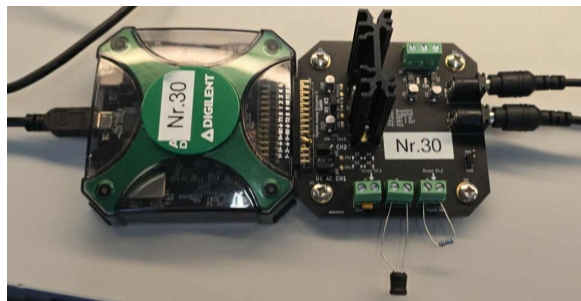


Figure 5: The RLC-circuit with one of the constellations of resistor, inductor and capacitor.

To analyze the behavior of the RLC circuit, a Digilent Analog Discovery device was used to both measure and control voltage signals. This device allows precise voltage signals to be generated and their response across the RLC circuit to be observed, using a Matlab code. Additionally, a printed circuit board was utilized to amplify the Matlab generated signal before it reached the RLC circuit. This setup allowed the transmission of signals and how the signals were influenced by the selected components.

When working with the electrical circuit, the following components were used:

$$C = 10,5\mu F$$

$$L = 4,5mH$$

These component values were selected after encountering difficulties during the initial measurements. The first capacitor produced a very high natural frequency, which made it difficult to collect the data accurately due to MatLab's limited sampling rate. To address this problem, a capacitor with a larger capacitance was chosen, lowering the natural frequency and allowing more reliable measurement to be taken. Measurements were taken across the capacitor, as its voltage provides the clearest representation of the circuit's behavior.

The input frequency affects the impedance of the components. For an RLC-circuit in series a low frequency results in a high capacitive reactance and a low inductive reactance, and low current. At resonant frequency, the capacitive reactance and inductive reactance are the same. Furthermore, if the frequency is high, inductive reactance is high, capacitive reactance is high and the overall impedance in the circuit is high. The terms 'high' and 'low' frequency are used to indicate whether the frequency is higher than, or lower than the resonant frequency.

Determining Resistance for Critical Damping

To properly interpret the measured signals, it is important to understand the theoretical behavior of the RLC circuit. The damping of the system is primarily determined by the resistor, and for the fastest non-oscillatory response, the circuit must be critically damped. Due to this, the differential equation is examined to determine the resistance value that results in critical damping.

The given second-order differential equation for an RLC circuit is:

$$\frac{d^2i(t)}{dt^2} + \frac{R}{L} \frac{di(t)}{dt} + \frac{1}{CL} i(t) = 0$$

In this equation, $\omega_0^2 = \frac{1}{CL}$ is the natural frequency of the circuit and $\gamma = \frac{R}{L}$ is the damping coefficient, which determines how quickly oscillations decay due to resistance.

In order to reach critical damping, the discriminant d in the equation must be equal to zero. The discriminant is derived from the quadratic form of the differential equation:

$$D = b^2 - 4ac$$

For critical damping to occur, we set $d = 0$:

$$\gamma^2 - 4\omega_0^2 = 0$$

From this equation, we derive the critical damping condition for γ :

$$\gamma = 2\omega_0$$

Substituting the definitions for γ and ω_0 :

$$\frac{R}{L} = 2\sqrt{\frac{1}{CL}}$$

In order to isolate R , we multiply both sides by L :

$$R = 2L\sqrt{\frac{1}{CL}}$$

Simplifying the equation, we get:

$$R = 2\sqrt{\frac{L^2}{CL}} = 2\sqrt{\frac{L}{C}} \quad (29)$$

In order to obtain an accurate value for the critical resistance, the actual values of the inductor and capacitor must be taken into consideration, as component tolerances can cause the measured values to deviate from the labeled values. Therefore, the precise values of the components were determined using an LCR meter before calculating the required resistance, as seen in figure 6.

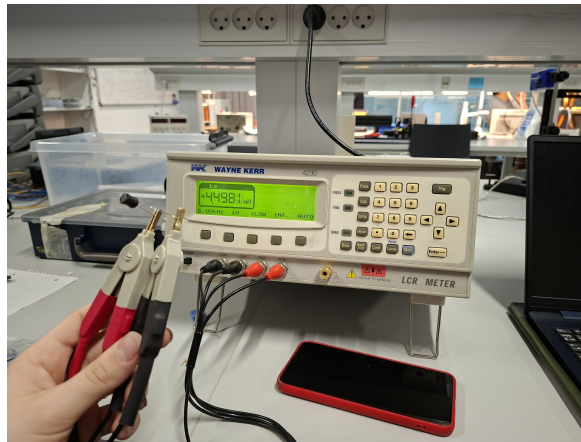


Figure 6: Example of how an LCR-meter was used to measure the precise value of components. In this example the precise inductance of an inductor was measured.

The measured component values for the RLC circuit are as follows:

- Inductor, $L = 4,5 \text{ mH} = 4,5 \cdot 10^{-3} \text{ H}$
- Capacitor, $C = 10,5 \mu\text{F} = 10,5 \cdot 10^{-6} \text{ F}$

Substituting these values into equation (29), and calculating the square root, we get:

$$R_{\text{critical}} = 2 \cdot \sqrt{\frac{4,5 \cdot 10^{-3}}{10,5 \cdot 10^{-6}}} = \sqrt{428,57} \approx 20,7$$

Multiplying by 2, we get:

$$R_{\text{critical}} = 2 \cdot 20,7 \approx 41,4 \Omega$$

The calculated critical resistance required for the RLC circuit to be critically damped is $41,4 \Omega$. Using a multimeter the internal resistance of the capacitor and inductor was measured to $16,5 \Omega$. Therefore we need an additional resistance of about:

$$41,4\Omega - 16,5\Omega = 24,9\Omega \quad (30)$$

The $24,9 \Omega$ would be required to achieve critical damping. When the resistance is less than $41,4 \Omega$, the circuit becomes underdamped and oscillates with a decreasing amplitude before gradually settling to equilibrium. Contrarily, if the resistance exceeds $41,4 \Omega$, the circuit becomes overdamped. This results in a slow response where the system approaches its steady state without any oscillations.

7 Results

7.1 Mechanical results

In this section, the results of the mechanical oscillations are presented, demonstrating different damping behaviors observed during the experiment. The oscillations are categorized into three different types: overdamped, critically damped, and underdamped. The data for these oscillations were gathered using Pasco Capstone, a data acquisition system, and further processed in MatLab.

Figure 7 shows the experimental results for each damping type, with each curve representing a different magnet size.

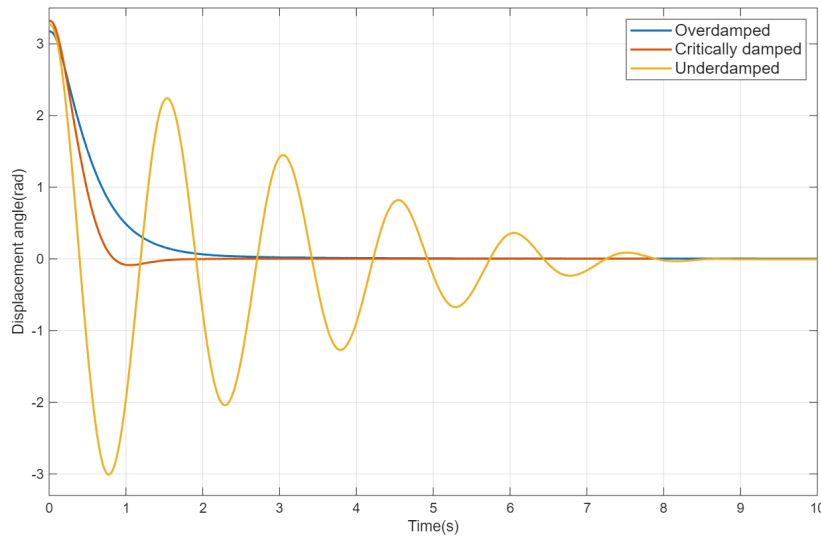


Figure 7: Mechanical oscillations: Experimental damping types. Colorcode: Blue=overdamped; largest magnet used, Orange=example of critically damped; medium magnet used, Yellow=underdamped; smallest magnet used.

The blue line represents the case of an overdamped oscillation, which occurs using the largest magnet. Overdamped oscillations are characterized by exponential decay, resulting from a large damping coefficient. Therefore, using the largest of our provided magnets was in order.

The orange line represents an approximately critically damped oscillation, which was obtained using a magnet of medium magnitude in order to achieve a damping coefficient of the appropriate size. A critically damped oscillation is characterized by the fastest way an oscillating system is driven to a halt without oscillating. Finding the exact damping value that achieves this fastest halt is highly impractical. Therefore, the graph above shows only an approximation of a critically damped system.

The yellow line represents an under damped oscillation, which was obtained using the smallest of the provided magnets to get a small damping coefficient. Under damped oscillations are characterized by a sinusoidal wave pattern with multiple peaks before eventually coming to a stop, as seen in figure 7.

These results demonstrate the impact of magnet size on the system's damping behavior.

The impact of Magnetic Damping

To further examine how magnetic damping influences the system, the oscillations were then measured under continuous external driving. By keeping the magnet size constant and varying the distance between the magnet and the disc, different damping strengths were achieved while minimizing the changes done to other system parameters. The resulting behavior can be seen in Figure 8.

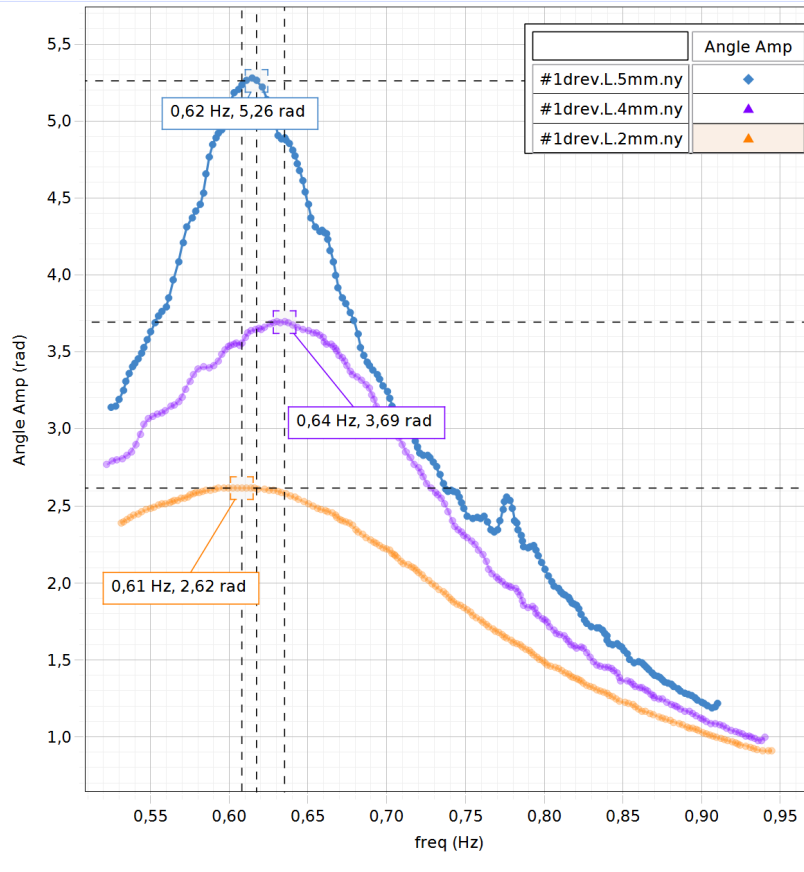


Figure 8: Mechanical oscillations: Resonant frequencies of driven oscillations with different magnetic dampings. The same magnet was used, but with different distances to the disc. Colorcode: Blue=5mm distance, Purple=4mm distance, Orange=2mm distance.

The data behind figure 8 were achieved by performing a sweep in which the driving frequency was lowered over time. This procedure was used to determine the exact driving frequency that matches the natural frequency of the system, thereby resulting in resonance, which is characterized by increased oscillation amplitude.

The blue dataset represents driven oscillations achieved using the smallest magnet at a distance of 5 mm from the disc and therefore represents the smallest amount of damping among the datasets shown in the graph. The resonant frequency of the blue dataset occurs at the peak of the curve, at 0,62 Hz. Due to varying sources of error the inconsistency around 0,77 Hz can be ignored.

The purple dataset represents the driven oscillations achieved with the smallest magnet with a distance of 4 mm from the disc, resulting in a larger damping coefficient than the blue data set. Here the resonant frequency is found at 0,64Hz.

The orange dataset represents the driven oscillations achieved with the smallest magnet with a dis-

tance of 2 mm from the disc, resulting in the largest damping coefficient among the three datasets. As the damping increases, the resonant peak occurs at a lower angular amplitude, which is characteristic for an increased damping. The resonant frequency in this case is 0,61Hz.

In general, the damping coefficient broadens the resonant peak of the curve. As the damping increases, the peak shifts further leftward. Additionally, greater damping results in smaller oscillations and therefore a smaller increase in angular amplitude when the resonance frequency is reached.

Using the same experimental setup, the behavior of the systems was then studied using free oscillations, as shown in figure 9.

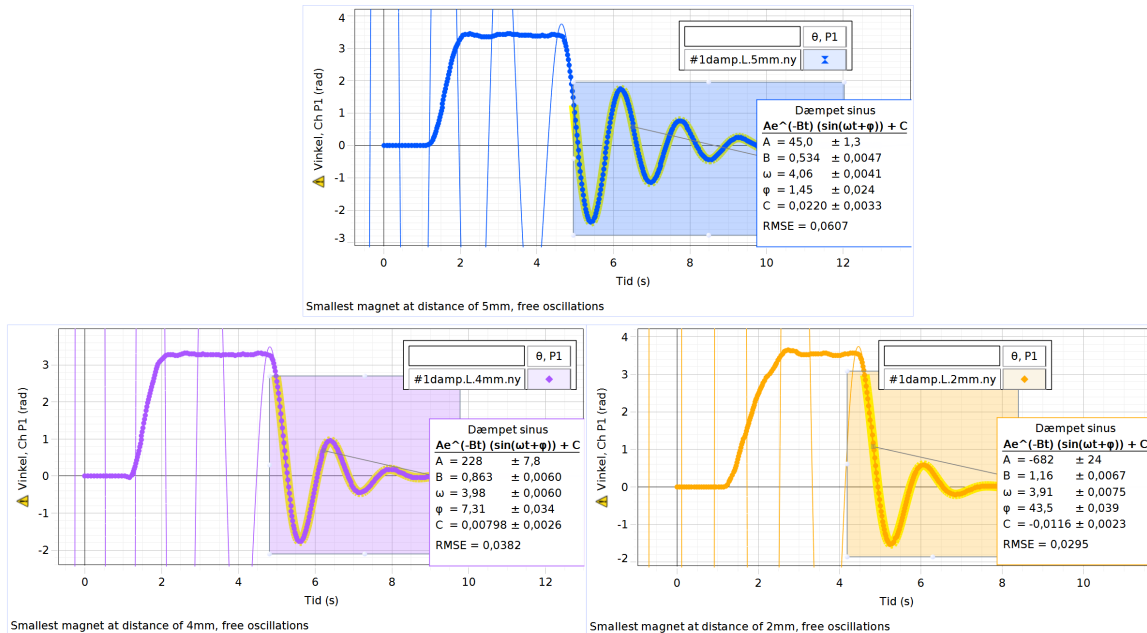


Figure 9: Mechanical oscillations: Damped sinus curve fit on free oscillations. Same magnet used. Colorcode: Blue=5mm distance, Purple=4mm distance, Yellow=2mm.

The colors used in figure 9 correspond to the same setups from the frequency sweep shown in figure 8. The system were allowed to oscillate freely, in order to determine the natural frequency and damping coefficient. The damping coefficient, represented by the letter B in the curve fit, is lowest in the blue graph (0,534), greater in the purple graph (0,863) and greatest in the orange graph (1,16), as expected. Although the natural frequency parameter ω in the curve fit is roughly the same across the datasets, it appears to decrease slightly with increased damping.

The natural frequency of the system is described by $\omega_0^2 = \frac{k}{I}$ and is theoretically independent of damping. However, since the entire system is influenced by damping, there is a slight change in its overall behavior. Given that the spring constants and inertia remain unchanged, this variation is minimal. The natural frequency obtained from the fits are as follows: Blue($\omega = 4,06\text{Hz}$), Purple($\omega = 3,98\text{Hz}$) and Orange($\omega = 3,91\text{Hz}$).

The impact of rotational Inertia

To then analyze the effect of rotational inertia on driven mechanical oscillations, the system's rotational inertia was varied while measuring its resonance frequencies. By adding different masses to the rotating disc, changes in both the resonant frequency and damping were to be expected, since the system's natural frequency is inversely proportional to the square root of its moment of inertia.

Figure 10 shows the resulting resonance curves for two different moments of inertia, which was accomplished by performing a similar driver-frequency sweep as in figure 8.

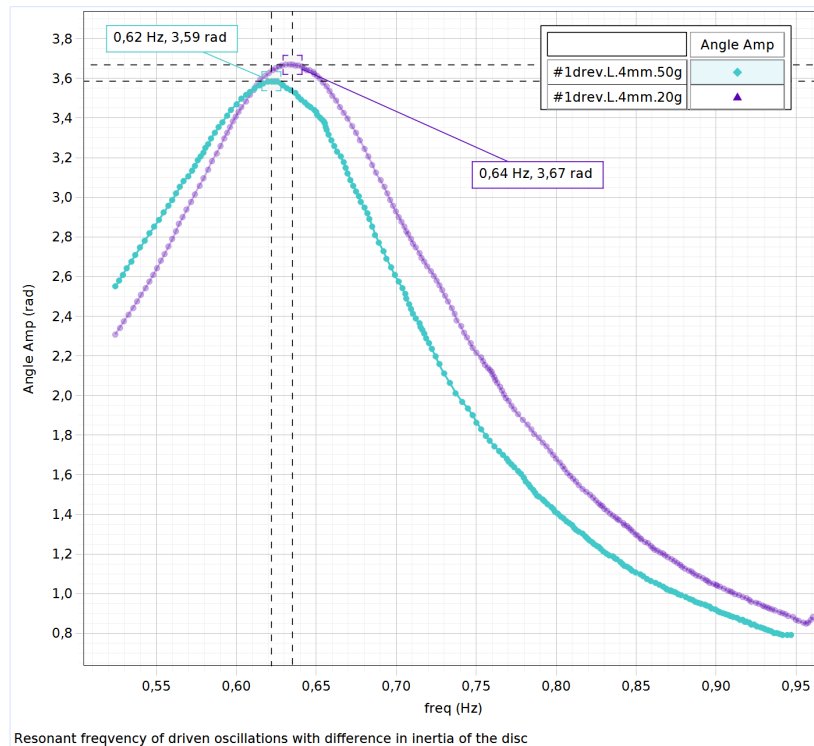


Figure 10: Mechanical oscillations: Resonant frequencies of driven oscillations with difference in rotational inertia. The moment of inertia was changed by adding weight to the disc and letting the magnet be untouched. Colorcode: Purple=20gr added, Turquoise=50gr added.

The purple curve represents a driven oscillation measured with the smallest magnet positioned at a distance of 4 mm from the disc and an added weight of 20 *gram*, resulting in a moment of inertia of 0,00016 $kg \cdot m^2$. The corresponding resonant frequency is found at 0,64 Hz.

The turquoise curve represents the driven oscillations measured with an added weight of 50 *gram*, increasing the moment of inertia to 0,000194 $kg \cdot m^2$. The resonant frequency of the turquoise curve occurs at 0,62 Hz.

Although the two curves are very similar, a slight shift can be observed. The purple graph is shifted towards a higher resonant frequency. The change is small which is expected given that the added mass causes only a small change in the moment of inertia. The purple graph shows a slightly less damped resonance, but according to equation (5) the rotational inertia and the damping are inversely proportional, and the opposite result is expected. This concept will be explored in figure 11.

While the resonance curves in figure 10 illustrate how changes in the rotational inertia affect the system under driven oscillations, they do not directly reflect the damping and natural frequency of the system. To analyze these properties, the same two rotational inertia configurations were therefore examined under free oscillation. This allows the damping coefficient and natural frequency to be determined independently of the external driving force, providing a clearer comparison of how the additional moment of inertia influences the system's behavior.

Figure 11 illustrates the data retrieved using the same setup from figure 10, this time as the systems oscillate freely. For clarity, the purple curves in figures 10 and figure 11 correspond to the same configuration, and likewise the turquoise curves represent the same setup in both figures.

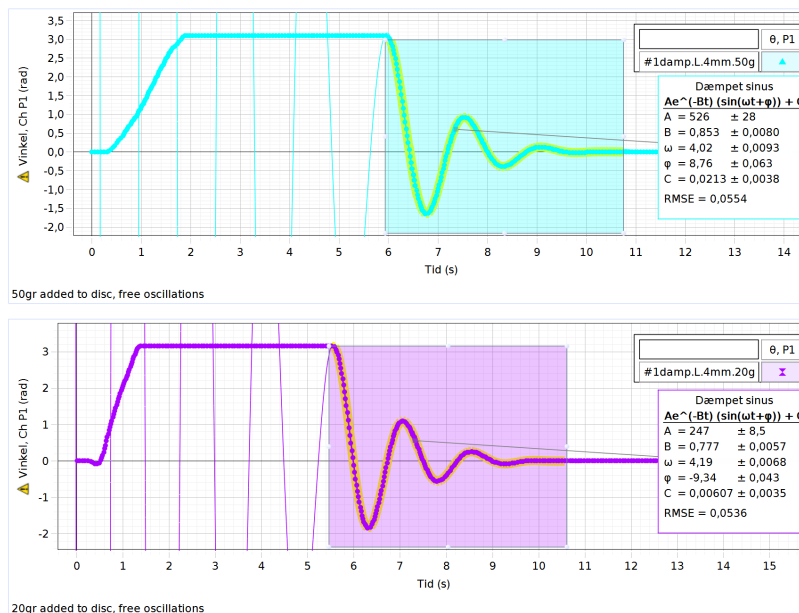


Figure 11: Mechanical oscillations: Damped sinus curve fit on free oscillations with difference in rotational inertia. The moment of inertia was changed by adding weight to the disc and letting the magnet be untouched. Colorcode: Purple=20gr added, Turquoise=50gr added.

The damping coefficient is given by the parameter B from the curve fit. It is lowest for the purple graph (0,777) and highest for the turquoise graph (0,853), although the opposite would initially be expected. While the magnet and its distance remained unchanged, the internal friction of the system was increased due to the added mass on the rotating disc. Therefore, the damping coefficient is found to increase with the increasing of the inertia, as the additional mass amplifies the internal friction within the system.

Since the natural frequency of the system is given by $\omega_0^2 = \frac{k}{I}$, where I is the moment of inertia, any change in inertia also influences the natural frequency of the system. In the curve fitting, the natural frequency is represented by ω , and determined to be: Turquoise ($\omega = 4,02\text{Hz}$) and Purple ($\omega = 4,19\text{Hz}$). These results show that increasing the moment of inertia leads to a decrease in the natural frequency, which is consistent with their inverse proportional relationship.

To revisit the increase in resonant frequency from the driven oscillations in figure 10, this can be explained by the increase in natural frequency. Seeing as the natural frequency increases as expected the resonant frequency must follow. The resonant frequency is a representation for the needed external frequency to bring the oscillating system to the greatest amplitude of oscillations.

7.2 Electronic results

Using the circuit components accounted for in section 6.2, the electrical experiments were then performed, starting with the free oscillations under varying damping conditions. This was achieved by applying a single square signal to the system and observing the resulting response once the input signal was shut off.

The objective of this experiment was to identify under damped, overdamped, and approximately critically damped responses in the electrical system. To achieve the desired responses, the roots of the second-order differential equation describing the circuit were examined. Theoretically, a damping coefficient of zero would result in undamped oscillations. However, this condition cannot be achieved, as some degree of damping would always be present in the system due to internal resistance within the circuit components. To achieve the smallest possible damping, the circuit was shorted at the resistance port, resulting in a damped oscillation. This behavior can be seen in figure 12 symbolized as the orange line, which shows oscillations that gradually decay over time as the system returns to equilibrium.

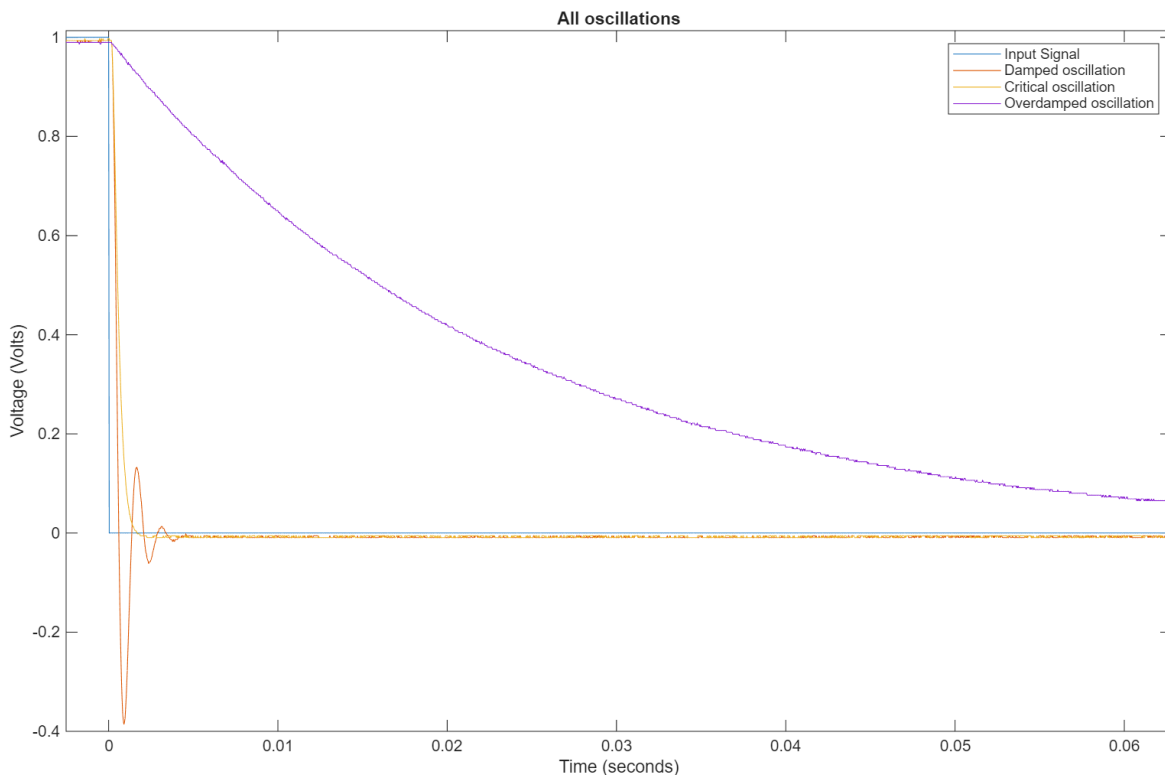


Figure 12: The blue line shows the input signal, the orange line shows the damped oscillations, the yellow line shows the approximated critical oscillation and the purple one shows the overdamped oscillation. This figure shows the different types of oscillations for our electrical system.

Figure 12 also illustrates the responses obtained under increased damping conditions on the system. By adding a resistance of 30Ω , an approximation of the critically damped condition was achieved. This response, represented by the yellow line, exhibits no oscillations and returns to equilibrium in the shortest amount of time. The absence of oscillations occurs due to the fact that a critically damped system produces the steepest possible slope in the measured signal without overshooting.

This can be seen from the solution to the equation, in which the damping coefficient squared is equal to four times the natural frequency. The system response then takes the form: $(Ax + Bt)e^{rt}$. The presence of the additional t term in the solution results in a faster decay toward equilibrium. It's important to note that this cannot be guaranteed to represent the exact critical damping of the system, but serves as a reasonable approximation.

When the damping is increased beyond this point, the system becomes overdamped. This causes the slope of the measured signal to become less steep, indicating a slower response. To clearly show this effect, a very high resistance value was chosen, which can be seen by the purple curve in figure 12.

The driven electrical circuit was then examined by performing a frequency sweep while measuring the phase shift. By placing a short circuit across the resistor port, the only resistance in the system came from the inductor and capacitor, which was $16,5\Omega$. The results can be seen in figure 13.

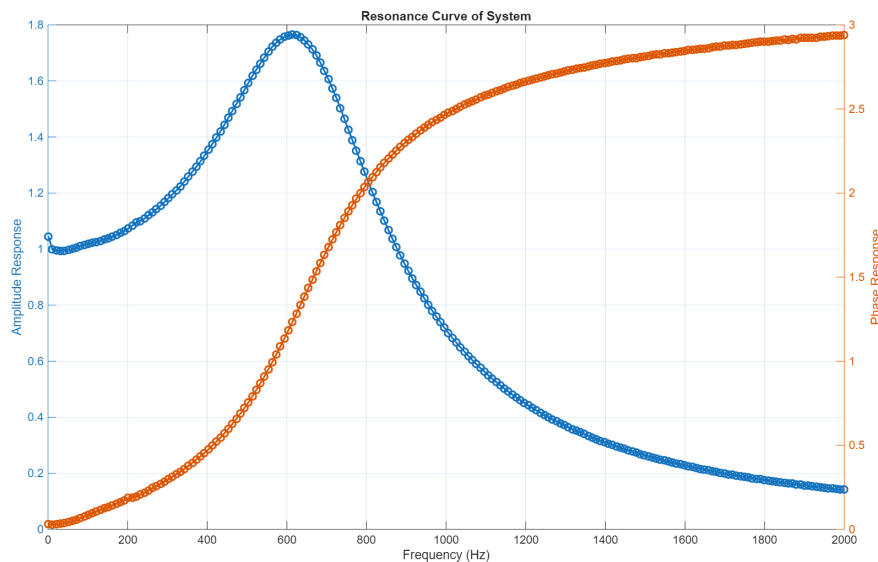


Figure 13: Resonance with internal resistance. Blue curve shows amplitude resonance. Orange curve shows how the phase shifts. X-axis shows the frequency of the input signal.

As shown in figure 13, the resonant frequency is around 600 Hz. Near this frequency, the phase shift is close to $\frac{\pi}{2}$. For a system with no resistance, resonance occurs when the driving force is in phase with the system's velocity, which corresponds to a phase shift of $\frac{\pi}{2}$. The measured resonant frequency being close to this value is therefore expected, since the resistance in the system is small.

To observe the effect of added resistance, a 10Ω resistor was added to the circuit and the frequency sweep was repeated, as shown in figure 14. The increased damping reduces the maximum resonance and shifts it toward lower frequencies.

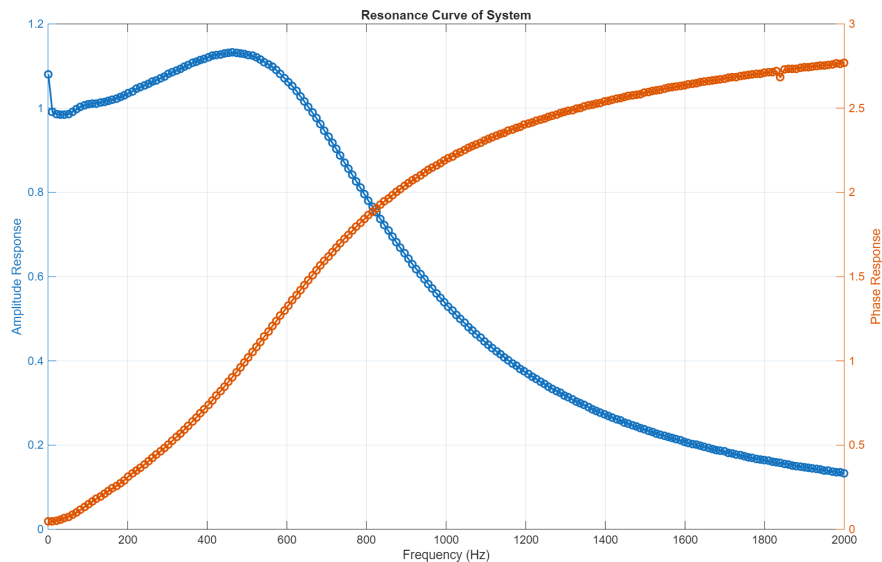


Figure 14: Resonance with total resistance of $26,5\Omega$. Blue curve shows amplitude resonance. Orange curve shows how the phase shifts. X-axis shows the frequency of the input signal.

The peak amplitude decreases from approximately 1,8 to 1,15, while the resonant frequency shifts from around 600Hz to 500Hz . The added damping also affects the phase response, making the phase shift less steep. As a result, the transition from being in phase to out of phase occurs more gradually.

7.3 Sources of error and measurement uncertainties

In the performed experiments, several sources of error and measurement uncertainties may have influenced the results and the accuracy of the obtained data.

One source of uncertainty comes from the equipment, as limited precision can lead to inaccuracies in measurements. At the same time, the theoretical framework assumes ideal systems, which do not fully reflect the case in practice. In the mechanical system, factors such as internal friction, air resistance, and imperfect mounting contribute to additional damping that is not accounted for theoretically. Similarly, the electrical system includes internal resistances and component tolerances, which have mainly been accounted for but still affect the system's behavior.

Overall, these sources of error and measurement uncertainties can explain minor deviations between the experimental results and the theoretical expectations. Nevertheless, the results remain consistent enough to support the expected outcomes. Future improvements would include collecting more data sets to increase the accuracy of the measurements, as well as minimizing the sources of experimental error.

8 Analogy between the two systems

Analogies are commonly used in science, whether to make abstract concepts more tangible or to compare seemingly unrelated subjects. Analogies are a valuable tool for understanding how different physical systems operate and relate to each other, and are often described using similar mathematical principles. However, two systems being analogous does not mean that they are identical; therefore,

it is important to be careful when attributing similarities.

The two equations describing the torsion pendulum and RLC circuit are:

$$\text{Mechanical : } \frac{d^2\theta(t)}{dt^2} + \frac{c}{I} \cdot \frac{d\theta(t)}{dt} + \frac{k}{I} \cdot \theta(t)$$

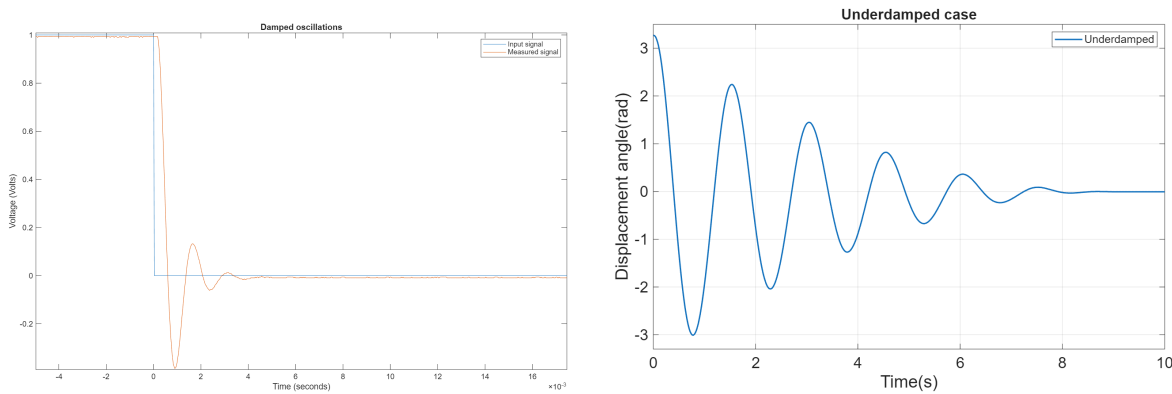
$$\text{Electrical : } \frac{d^2i(t)}{dt^2} + \frac{R}{L} \frac{di(t)}{dt} + \frac{1}{LC} i(t)$$

A clear similarity can be seen between these equations, which were derived independently from each other. Both are second-order differential equations. The angular displacement in the mechanical system corresponds to the current in the electrical system, the spring constant in the mechanical system corresponds to $\frac{1}{C}$ and the damping in the mechanical system corresponds to the resistance.

This is further supported by the results presented in section 7.2, where changes in resistance were shown to affect the system by increasing or decreasing damping. This confirms that the resistance parameter does in fact describe the damping of the system. The capacitance was varied in order to examine its effect on the natural frequency of the system.

In the mechanical system, section 7.1 examined the impact of rotational inertia of the system. This demonstrated that changes in the moment of inertia affect all system parameters, as the rotational inertia influences the entire system.

By changing these parameters, a clear correlation between the two systems is seen. Both systems can be described by the same linear second-order differential equation, and it is possible to substitute parameters when transitioning from one system to the other.



(a) Damped oscillations of the electrical circuit

(b) Damped oscillations of the mechanical system

Figure 15: Comparison between the damped electrical circuit and the damped mechanical system. figure (a) shows the electrical circuit. notice the x-axis in figure (a) as it is times 10^{-3} . Figure (b) shows the mechanical system.

Figure 15 illustrates that both systems exhibit the same oscillatory behavior, despite being different systems. It is important to state that the reason behind the difference in time scale is due to the difference in how the natural frequency is defined for each system. In the electrical system, the

natural frequency is given by $\sqrt{\frac{1}{CL}}$. Because the component values are very small, 10^{-9} , the natural frequency therefore becomes very large, resulting in rapid oscillations. In the mechanical system, the natural frequency is defined as $\sqrt{\frac{k}{I}}$, which does not lead to frequencies of the same magnitude and therefore results in slower oscillations.

9 Conclusion

To conclude, the aim of this report was to construct theoretical models for a torsion pendulum and RLC-circuit. It was found that both systems can be described using a linear second order differential equation. When working with the systems, both driven oscillations and free oscillations were examined. It was explored how changing the damping affected both systems. Here it was observed that, with some approximation, the behavior of both systems matched what had been theorized. In the torsion pendulum, the unexpected values could be explained to be caused by internal friction in the system.

Finally, an analogy of the two systems was explored. Looking at the differential equations for the two systems it was seen that the constituent variables of the equations were analogous. The resistor in the RLC-circuit was found to be comparable to the magnet in the mechanical system. Likewise, changing the capacitor in the electrical system was found to change the natural frequency of the system, and changing the inertia of the disc in the torsion pendulum affected the whole system.

If the experiments were to be repeated, some improvements we suggest are: Finding a way to control the damping in the mechanical system more precisely. This could be done by using a tool to measure the magnetic properties of the different magnets. The experiment regarding the impact of the inertia could be improved by adding more weight to the disc and by repeating the experiment, so that there would be more datasets to compare. In terms of the electrical system, the experiment could be improved by exploring impedance and internal resistance more accurately. Another way to improve our measurements for the electrical system, is to use a lock-in amplifier to find the amplitude and phase shift. This works by sending in a wave with a specific frequency, and thereby it is possible to find the signal of a electrical system, through all the noise. With this signal found we would be able to find the amplitude and phase shift of the given signal [4].

References

- [1] Robert Resnick & Jearl Walker David Halliday. *Principles of Physics: Extended, International Adaptation, 12th Edition*. John Wiley & Sons Inc, 2023.
- [2] Robert Adams & Christoffer Essex. *Calculus: A Complete Course, 10th Edition*. Pearson Education, 2021.
- [3] Allan R. Hambley. *Electrical Engineering: Principles & Applications, Global edition, 7th Edition*. Pearson Educated Limited, 2018.
- [4] Zurich Instruments. *Principles of Lock-in Detection*. URL: <https://www.youtube.com/watch?v=ZIjBRA2SONQ>. (accessed: 13.12.2025).